JOURNAL OF VIROLOGY, May 2011, p. 4122–4134 Vol. 85, No. 9
0022-538X/11/$12.00 doi:10.1128/JVI.02232-10

Evidence that TMPRSS2 Activates the Severe Acute Respiratory Syndrome Coronavirus Spike Protein for Membrane Fusion and Reduces Viral Control by the Humoral Immune Response▽

Ilona Glowacka,[1]† Stephanie Bertram,[1]† Marcel A. Müller,[2] Paul Allen,[3] Elizabeth Soilleux,[3] Susanne Pfefferle,[4] Imke Steffen,[1] Theodros Solomon Tsegaye,[1] Yuxian He,[5] Kerstin Gnirss,[1] Daniela Niemeyer,[2] Heike Schneider,[6] Christian Drosten,[2] and Stefan Pöhlmann[1,7]*

Institute of Virology, Hannover Medical School, 30625 Hannover, Germany[1]; Institute of Virology, University of Bonn Medical Centre, 53127 Bonn, Germany[2]; Department of Cellular Pathology, John Radcliffe Hospital, Oxford OX3 9DU, England[3]; Bernhard Nocht Institute for Tropical Medicine, 20359 Hamburg, Germany[4]; Institute of Pathogen Biology, Chinese Academy of Medical Sciences and Peking Union Medical College, Beijing 1007302, China[5]; Institute for Physiological Chemistry, Hannover Medical School, 30625 Hannover, Germany[6]; and German Primate Center, Kellnerweg 4, 37077 Göttingen, Germany[7]

Received 25 October 2010/Accepted 27 January 2011

The spike (S) protein of the severe acute respiratory syndrome coronavirus (SARS-CoV) can be proteolytically activated by cathepsins B and L upon viral uptake into target cell endosomes. In contrast, it is largely unknown whether host cell proteases located in the secretory pathway of infected cells and/or on the surface of target cells can cleave SARS S. We along with others could previously show that the type II transmembrane protease TMPRSS2 activates the influenza virus hemagglutinin and the human metapneumovirus F protein by cleavage. Here, we assessed whether SARS S is proteolytically processed by TMPRSS2. Western blot analysis revealed that SARS S was cleaved into several fragments upon coexpression of TMPRSS2 (*cis*-cleavage) and upon contact between SARS S-expressing cells and TMPRSS2-positive cells (*trans*-cleavage). *cis*-cleavage resulted in release of SARS S fragments into the cellular supernatant and in inhibition of antibody-mediated neutralization, most likely because SARS S fragments function as antibody decoys. *trans*-cleavage activated SARS S on effector cells for fusion with target cells and allowed efficient SARS S-driven viral entry into targets treated with a lysosomotropic agent or a cathepsin inhibitor. Finally, ACE2, the cellular receptor for SARS-CoV, and TMPRSS2 were found to be coexpressed by type II pneumocytes, which represent important viral target cells, suggesting that SARS S is cleaved by TMPRSS2 in the lung of SARS-CoV-infected individuals. In summary, we show that TMPRSS2 might promote viral spread and pathogenesis by diminishing viral recognition by neutralizing antibodies and by activating SARS S for cell-cell and virus-cell fusion.

The severe acute respiratory syndrome coronavirus (SARS-CoV) is the causative agent of the lung disease SARS, which claimed ~800 lives in 2002 to 2003 (49). SARS-CoV-related viruses were identified in bats and palm civets (19, 33, 37), and it is believed that human contact with the latter animals, possibly within animal markets in southern China, was responsible for the introduction of SARS-CoV into the human population. The viral spike (S) protein mediates infectious entry into target cells by engaging the carboxypeptidase angiotensin-converting enzyme 2 (ACE2) (36, 60), and several changes in the spike sequence of SARS-CoV from humans relative to SARS-CoV from palm civets reflect the adaptation to efficient usage of the human receptor (35, 38, 39), most likely a prerequisite for high viral pathogenicity. Thus, the SARS S protein is an important determinant of viral cell and species tropism (27), and exploration of its functions is essential to devise effective strategies for prevention and therapy.

The SARS S protein comprises 1,255 amino acids and harbors 23 consensus sequences for N-linked glycosylation. The S protein is synthesized in the secretory pathway of infected cells, and S protein trimers are incorporated into the viral envelope (derived from the endoplasmic reticulum Golgi intermediate compartment [ERGIC]) and the plasma membrane of the host cell (34). The S protein exhibits the domain organization of class I fusion proteins; it contains an N-terminal surface unit (S1), which engages the receptor, and a C-terminal transmembrane unit (S2), which contains the membrane fusion machinery (27). A prominent feature of many class I fusion proteins is the requirement for proteolytic activation by host cell enzymes (14). A seminal study by Simmons and colleagues showed that proteolytic activation of SARS S is mediated by cathepsins in target cells, most importantly by cathepsin L (53). In contrast, the efficiency and biological relevance of SARS S processing by proteases in infected cells is at present incompletely understood.

The type II transmembrane serine protease TMPRSS2 has recently been shown to proteolytically activate the fusion pro-

* Corresponding author. Mailing address: Infection Biology Unit, German Primate Center, Kellnerweg 4, 37077 Göttingen, Germany. Phone: 49 551 3851 150. Fax: 49 551 3851 184. E-mail: s.poehlmann@dpz.eu.

† I.G. and S.B. contributed equally to this work.

▽ Published ahead of print on 16 February 2011.

teins of human influenza viruses (6, 8), and TMPRSS2 was found to activate human metapneumovirus (51). In addition, the related protein TMPRSS11a has been demonstrated to cleave SARS S and to moderately increase viral infectivity (30). Here, we investigated whether SARS S is a substrate of TMPRSS2 and if cleavage modulates biological properties of SARS S-bearing viruses. We show that SARS S is proteolytically processed by TMPRSS2. Cleavage resulted in shedding of SARS S fragments and interference with antibody-mediated neutralization or in activation of SARS S for cell-cell and virus-cell fusion, depending on the presence of TMPRSS2 on SARS S-expressing cells or on adjacent susceptible cells. These observations, in conjunction with our finding that ACE2 and TMPRSS2 are coexpressed in type II pneumocytes, important viral target cells, suggest that TMPRSS2 might impact SARS-CoV spread by at least two independent mechanisms.

MATERIALS AND METHODS

Plasmid construction and *in vitro* mutagenesis. Expression plasmids pCAGGS-SARS-S, encoding the spike protein of SARS-CoV strain Frankfurt, and pcDNA3-hACE2, encoding human ACE2 (hACE2), have been described previously (25, 26). The plasmids encoding human TMPRSS2 and TMPRSS4 and mouse matriptase-3 have also been described previously (29, 51, 57).

Cell culture. Vero E6 and 293T cells were propagated in Dulbecco's modified Eagle's medium (DMEM) supplemented with 10% fetal bovine serum (FBS), penicillin, and streptomycin and were grown in a humidified atmosphere containing 5% CO_2. 293T cells stably expressing ACE2 (293T-hACE2) (18) were generated by transfection of plasmid pcDNA3.1zeo-hACE2 (25) into 293T cells, followed by selection of resistant cells with zeocin (Invitrogen) at 50 μg/ml. Homogenous surface expression of ACE2 on stably transfected cells was confirmed by fluorescence-activated cell sorting (FACS) analysis.

Production of lentiviral pseudotypes and infection experiments. For generation of lentiviral pseudotypes, calcium phosphate transfections were performed as described previously (26, 54). In brief, 293T cells were transiently cotransfected with pNL4-3 E-R- Luc (11), and expression plasmids for SARS S or the G protein of vesicular stomatitis virus (VSV-G). For some experiments, human TMPRSS2 or TMPRSS4 or mouse matriptase-3 was coexpressed during production of pseudotypes. The culture medium was replaced at 16 h and harvested at 48 h posttransfection. The supernatants were passed through 0.45-μm-pore-size filters, aliquoted, and stored at −80°C. For normalization of different virus stocks, capsid protein (p24) contents were determined using a commercially available kit (Murex, Wiesbaden, Germany). Alternatively, virus stocks were normalized for infectivity, which was assessed by infecting 293T-hACE2 cells with different dilutions of pseudotypes, followed by determination of luciferase activities in cell lysates by employing a commercially available kit (Promega, Madison, WI). For infection experiments, 293T-hACE2 cells were incubated with equal volumes of p24- or infectivity-normalized pseudotypes for 16 h. Thereafter, medium was changed, and luciferase activities in cell lysates were determined at 72 h postinfection. For inhibition experiments, cells were preincubated with the cathepsin inhibitor MDL 28170 (Calbiochem, Nottingham, United Kingdom) for 30 min, or viruses were preincubated with antiserum (obtained by immunization of mice with an S1 protein fragment comprising amino acids 12 to 327) (62) for 60 min before the addition to target cells. Culture supernatants were removed at 16 h postinfection and replaced by fresh medium without inhibitor. For some inhibition studies, the pseudotypes were first pelleted through a sucrose cushion by ultracentrifugation for 2 h at 25,000 rpm and 4°C to separate particles from SARS S fragments not associated with virions and then incubated with antiserum in the presence and absence of shed SARS S protein.

Production of VLPs. For production of virus-like particles (VLPs), 293T cells were cotransfected with the HIV-1 Gag (p55)-encoding plasmid p96ZM651gag-opt (16), SARS S expression plasmid, and expression plasmids for proteases or empty vector. The supernatants containing the VLPs were collected at 48 h posttransfection and concentrated by ultrafiltration using VivaSpin centrifugal concentrators (Sartorius, Aubagne Cedex, France). Alternatively or additionally, the VLPs were concentrated by ultracentrifugation through a 20% sucrose cushion for 2 h at 25,000 rpm and 4°C. Subsequently, the concentrated supernatants were treated with phosphate-buffered saline (PBS) or trypsin, followed by addition of soybean trypsin inhibitor (Sigma, Deisenhofen, Germany).

Production of shed SARS S protein. For production of shed SARS S protein, 293T cells were cotransfected with plasmids encoding SARS S and TMPRSS2 or empty vector. At 48 h posttransfection the supernatants were harvested and concentrated using VivaSpin columns (Sartorius, Aubagne Cedex, France), followed by ultracentrifugation through a 20% sucrose cushion for 2 h at 25,000 rpm and 4°C to remove vesicles harboring SARS S protein. The SARS S protein remaining in the supernatants of ultracentrifuged material was then analyzed by immunoblotting to confirm size and purity.

Detection of SARS S by immunoblotting. For Western blot analysis, lysed VLP preparations were separated by SDS-PAGE and transferred onto nitrocellulose membranes. SARS S protein was detected by staining with rabbit serum specific for the S1 subunit (generated by immunization with a peptide comprising SARS S amino acids 19 to 48) (24) or the S2 subunit (Imgenex, San Diego, CA). For a loading control, the stripped membranes were incubated with an anti-HIV p24 antibody.

PNGase F digest of SARS S. For the analysis of SARS S glycosylation, VLPs were concentrated via VivaSpin columns (samples taken for immunoblotting) and additionally ultracentrifuged through a 20% sucrose cushion at 25,000 rpm for 2 h at 4°C. The resulting pellets were harvested with TNE (Tris-HCl, 0.15 M NaCl, and 10 mM EDTA) buffer and digested by peptide *N*-glycosidase F (PNGase F; New England BioLabs, Frankfurt, Germany). The digested samples were then analyzed by immunoblotting as described above.

Immunohistochemistry. Tissue samples, obtained with full ethical approval from the National Research and Ethics Service (Oxfordshire Research and Ethics Committee A, reference 04/Q1604/21), were stained with hematoxylin and eosin using standard techniques and were immunostained for ACE2 (affinity purified goat polyclonal serum; R&D Systems, Abingdon, United Kingdom), detected with biotinylated secondary donkey anti-goat polyclonal antiserum (Abcam, Cambridge, United Kingdom) and the Bond Intense R kit (Leica Microsystems Newcastle Ltd., Newcastle, United Kingdom), or for TMPRSS2 (mouse monoclonal antibody P5H9) (41) using the manufacturer's standard protocols and reagents for mouse primary antibodies. Immunostaining was performed using a Bond Max immunostaining machine (Leica Microsystems Newcastle Ltd., Newcastle, United Kingdom). As a negative control for ACE2 immunostaining, normal goat polyclonal serum was substituted for the primary antibody. As a negative control for TMPRSS2 immunostaining, an irrelevant mouse monoclonal antibody (anti-melan A antibody, clone A103; Leica Microsystems Newcastle Ltd., Newcastle, United Kingdom) was substituted for the primary antibody. Stained sections were photographed with a Nikon DS-FI1 camera with a Nikon DS-L2 control unit (Nikon United Kingdom Limited, Kingston-upon-Thames, United Kingdom) and an Olympus BX40 microscope (Olympus UK Limited, Watford, United Kingdom).

Quantitative reverse transcription-PCR (RT-PCR) analysis of TMPRSS2 mRNA expression. For detection of *Tmprss2* transcripts by real-time PCR, an ABI 7500 FAST real-time PCR system (Applied Biosystems, Carlsbad) was used. The PCR mixtures contained 0.5 μl of cDNA (Clontech, Saint-Germain-en-Laye, France) in a total volume of 10 μl. Specific amplification was ensured with TaqMan gene expression assays (catalog number 4331182; Applied Biosystems), which were used according to the manufacturer's recommendations. The following specific assays were used: Hs00237175_m1 (TMPRSS2) and Hs99999908_m1 (β-glucuronidase [GUSB]). The average cycle threshold value (C_T) for each individual assay was calculated from triplicate measurements by means of the instrument's software in the auto C_T mode (7500 FAST System Software, version 1.3.0). Average C_T values calculated for TMPRSS2 were normalized by subtraction from the C_T values obtained for GUSB (housekeeping reference). Template-free cDNA reactions were analyzed in parallel using both TaqMan assays; no specific signal was detected in any of these experiments.

***trans*-cleavage of SARS S by TMPRSS2.** In order to determine if SARS S on the cell surface can be cleaved by TMPRSS2 on neighboring cells (*trans*-cleavage), 293T cells were transfected with plasmids encoding SARS S, TMPRSS2 or TMPRSS4, or empty vector. At 24 h posttransfection the cells were resuspended in fresh FCS-free DMEM, and cells expressing SARS S were mixed with cells expressing empty vector or protease at a ratio of 1:1.7. The mixed cells were seeded again in new cell culture flasks for further incubation for 30 h at 37°C. Subsequently, the supernatants were harvested, centrifuged for 5 min at 4,000 rpm, passed through a 0.45-μm-pore-size filter, and concentrated by ultrafiltration using VivaSpin centrifugal concentrators (Sartorius, Aubagne Cedex, France). Additionally, the concentrated supernatants were loaded on a 20% sucrose cushion and ultracentrifuged for 2 h at 25,000 rpm and 4°C. After ultracentrifugation, the supernatants were harvested, and the pellet was resuspended in TNE buffer. To analyze SARS S cleavage, lysates of transfected cells and samples of supernatants taken during the different processing steps were

analyzed for the presence of SARS S by Western blotting, employing sera specific for the S1 and S2 subunits of SARS S.

SARS S-driven cell-cell fusion. For analysis of SARS S-driven cell-cell fusion, 293T effector cells seeded in six-well plates at 1.2×10^5 cells/well were $CaPO_4$ transfected with either an empty pCAGGS plasmid or pCAGGS encoding SARS S in combination with plasmid pGAL4-VP16, which encodes the herpes simplex virus VP16 transactivator fused to the DNA binding domain of the *Saccharomyces cerevisiae* transcription factor GAL4. In parallel, 293T target cells were seeded in 48-well plates at 0.8×10^5 cells/well and transfected with pcDNA3 or the hACE2 expression vector or with a protease-expressing vector together with plasmid pGal5-luc, which encodes the luciferase reporter gene under the control of a promoter containing five GAL4 binding sites. The day after transfection, effector cells were diluted in fresh medium and added to the target cells. For trypsin treatment, medium from target cells was completely removed, and effector cells in medium supplemented with 100 ng/ml trypsin (Sigma, Deisenhofen, Germany) or PBS were added. After a 6-h incubation, fresh medium was added to the trypsin- and PBS-treated samples. Cell-cell fusion was quantified by determination of luciferase activities in cell lysates 48 h after cocultivation using a commercially available kit (Promega, Madison, WI).

TMPRSS2-dependent syncytium formation. Vero E6 cells (seeded in a six-well plate at 6×10^5 cells/well) were Lipofectamine transfected with TMPRSS2 or TMPRSS4 expression plasmid or control transfected with empty vector. After 24 h cells were infected with SARS-CoV (strain Frankfurt 1) at a multiplicity of infection (MOI) of 0.1 for 1 h at 37°C. Subsequently, the cells were washed, and fresh culture medium was added. At 29 h postinfection, the cells were fixed with paraformaldehyde (8%) and analyzed by microscopy. Pictures were taken with a Zeiss phase-contrast inverted microscope (Televal 31) at a 200-fold magnification.

TMPRSS2-dependent, cathepsin-independent cellular entry of SARS-CoV. 293T-hACE2 cells (seeded in a six-well plate at 6×10^5 cells/well) were transfected in triplicates with expression plasmids encoding TMPRSS2 or TMPRSS4 or control transfected with empty vector. After 24 h transfected cells were incubated with either DMEM containing the cathepsin inhibitor MDL 28170 (stock solution prepared in dimethyl sulfoxide [DMSO]) at a final concentration of 9 μM or DMEM containing the same volume of DMSO (as negative control) for 60 min at 37°C. Subsequently, the cells were infected with SARS-CoV (Frankfurt strain 1) at an MOI of 0.1 for 30 min at 4°C, washed twice with PBS, and incubated with fresh DMEM. At 5 h postinfection the cells were washed with PBS and lysed, and total RNA was extracted by an RNeasy Protect Mini kit (Qiagen, Hilden, Germany). SARS-CoV entry was determined by quantitative RT-PCR specific for the subgenomic mRNA (sgmRNA) of the N transcript. For this, the oligonucleotides SsgN-F (AACCTCGATCTCTTGTAGATCTGT), SsgN-R (TGAATCTGTGGGTCCACCAA), and SsgN-P (FAM-CTCTAAACG AACAAATTAAAATGTCTGATAATGG-BHQ1, where FAM is 6-carboxyfluorescein and BHQ1 is Black Hole quencher 1) were used with a SuperScript III One-Step RT-PCR kit (Invitrogen). The total reaction mixture volume was 12.5 μl (quarter reaction), and the mixture contained 30 nmol of $MgSO_4$, 5 pmol of each oligonucleotide, and 2.5 pmol of the probe. The C_T values, measured in single experiments performed in triplicates, were normalized by subtracting the respective C_T value for the TATA-box binding protein (housekeeping reference gene) (50). For clarity, values were subtracted by a fixed number (20). A C_T difference of 3 correlated approximately with a 10-fold increase as determined by a dilution series of both targets.

RESULTS

The pulmonary protease TMPRSS2 cleaves SARS S at multiple sites. Recent studies showed that TMPRSS2, TMPRSS4, and other type II transmembrane serine proteases (TTSPs) can activate human influenza viruses (6, 8, 10). Since the lung is also the major target organ of SARS-CoV, we asked whether TMPRSS2 and TMPRSS4 can cleave the SARS S protein. We included murine matriptase-3 in these experiments since we previously found that this protease was unable to process influenza virus hemagglutinin (HA) and would thus serve as a negative control (8). Employing an S2-specific antibody, Western blot analysis of virus-like particles (VLPs) released from transiently transfected cells revealed a prominent 160- to 170-kDa band representing full-length SARS S, and, upon trypsin treatment, a 90-kDa band representing S2 (Fig. 1, top panel), in agreement with published data (3, 67). When TMPRSS2 and S protein were coexpressed, the largest band observed was approximately 150 kDa (instead of the 160 kDa expected for full-length SARS S), with additional bands of 45, 55, and 85 kDa (Fig. 1, top panel). In contrast, coexpression of TMPRSS4 or matriptase-3 did not facilitate SARS S cleavage.

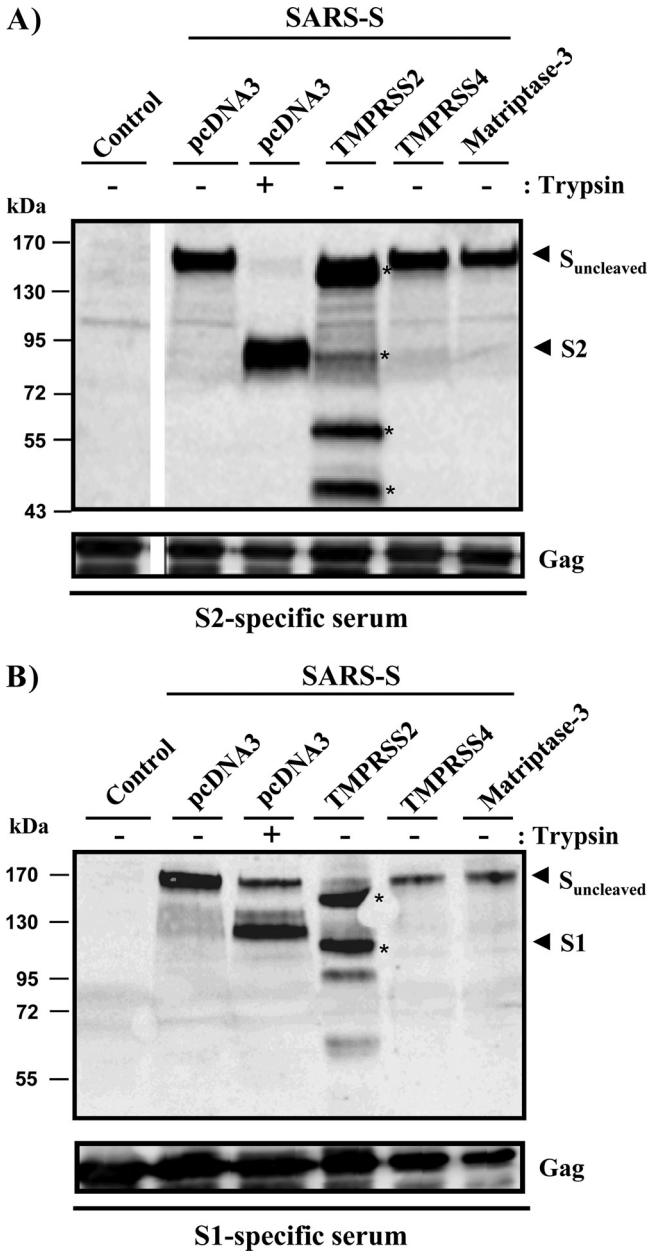

FIG. 1. Proteolytic processing of SARS S by TMPRSS2. (Top) VLPs were produced by coexpression of HIV p55 Gag and SARS S in the absence and presence of coexpressed human TMPRSS2, TMPRSS4, or murine matriptase-3, treated with trypsin or PBS, and analyzed for S protein and HIV p55 Gag content as indicated, using a serum specific for the S2 subunit of SARS S. (B) The experiment was carried out as described for panel A. However, an S1-specific antiserum was used for SARS S protein detection.

Efficient proteolytic processing of SARS S by TMPRSS2 was

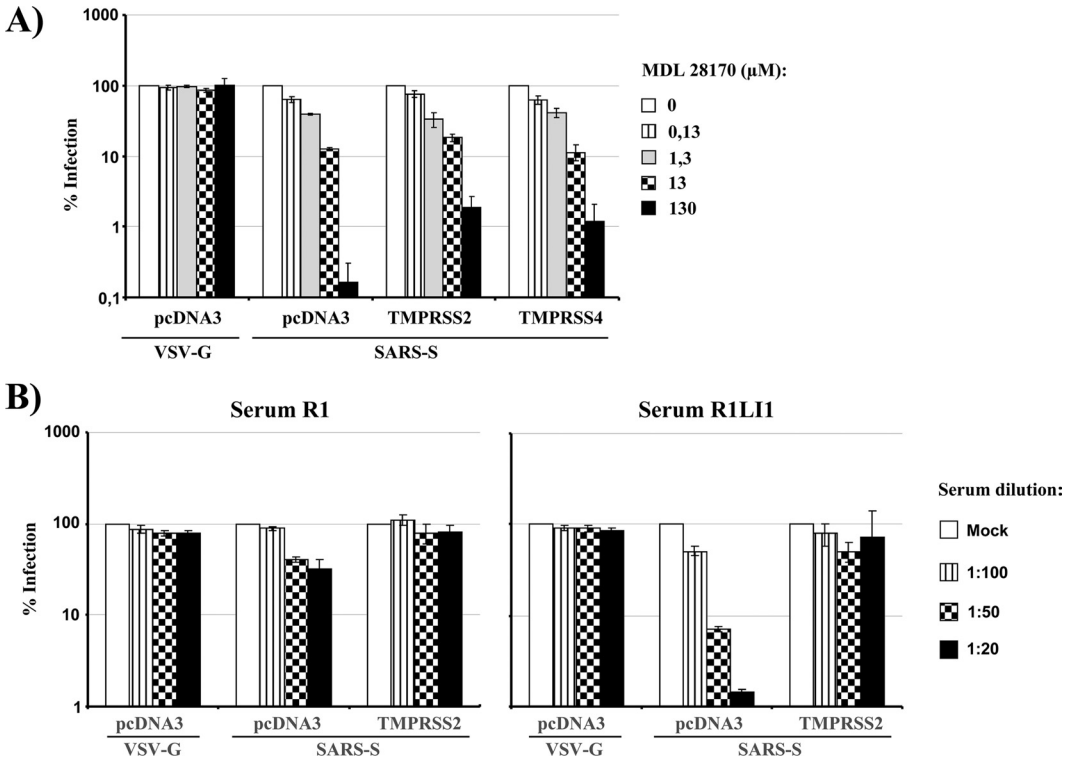

FIG. 2. Impact of SARS S processing by TMPRSS2 on cathepsin dependence and neutralization sensitivity. (A) 293T cells engineered to express large amounts of ACE2 were incubated with the indicated concentrations of the cathepsin B/L inhibitor MDL 28170 and inoculated with pseudotypes in triplicate, and luciferase activities were determined at 72 h postinfection. Activities measured in the absence of inhibitor were set as 100%. A representative experiment out of three is shown; error bars indicate standard deviations. In the absence of inhibitor, the following luciferase counts were measured: VSV-G, 55,642 ± 4877 cps; SARS S plus pcDNA3, 64,751 ± 11,505 cps; SARS S plus TMPRSS2, 59,071 ± 5,087 cps; SARS plus TMPRSS4, 94,684 ± 4,576 cps. (B) Equal volumes of pseudotypes bearing SARS S wt were incubated for 60 min with the indicated dilutions of the sera R1 and R1LI1 in triplicate and then added to ACE2-expressing 293T cells. Luciferase activities in cell lysates were determined after 72 h, and activities measured in the absence of serum were set as 100%. The results ± standard deviations of a representative experiment are shown. Similar results were obtained in two independent experiments. In the absence of serum, the following luciferase counts were measured: VSV-G, 9,037,372 ± 33,0551 cps; SARS-S plus pcDNA3, 5,411,448 ± 304,990 cps; SARS-S plus TMPRSS2, 444,923 ± 27,314 cps.

confirmed when an S1-specific serum was used for S protein detection (Fig. 1, bottom panel). Thus, SARS S fragments of 100 and 150 kDa were observed upon coexpression of SARS S with TMPRSS2 while only a single, 160-kDa band was detected when SARS S was produced in cells cotransfected with empty vector instead of the TMPRSS2 expression plasmid (Fig. 1, bottom panel). Cumulatively, TMPRSS2 cleaves SARS S at multiple sites, generating fragments of 150, 110, 85 (weak signal), 55, and 45 kDa.

SARS S cleavage by TMPRSS2 decreases viral sensitivity to inhibition by neutralizing antibodies. Considering that TMPRSS2 cleaves SARS S at multiple sites, we first asked if processed S protein was still active. For this, we employed lentiviral pseudotypes bearing SARS S, which faithfully model host cell entry of SARS-CoV (26, 55, 65). Analysis of infectivity of viruses produced in control- and TMPRSS2-transfected cells and normalized for equal content of p24 capsid antigen did not reveal major differences (data not shown), suggesting that cleavage of SARS S by TMPRSS2 was compatible with viral infectivity. We next investigated whether processing of SARS S by TMPRSS2 alleviated the requirement for cathepsin activity during infectious SARS S-dependent cell entry. Preincubation of 293T-hACE2 cells with a cathepsin L and B inhibitor, MDL 28170 (40, 53), had no effect on infectious entry of VSV-G-bearing pseudotypes but efficiently reduced infection by SARS S pseudotypes (Fig. 2A and raw data in the legend), in agreement with published results (28, 53). The pronounced reduction of infectivity of SARS S pseudotypes by MDL 28170 was not rescued by SARS S processing by TMPRSS2 (Fig. 2A), indicating that proteolysis of SARS S by TMPRSS2 does not abrogate the requirement for cleavage by cathepsin L and/or B.

The humoral immune response critically contributes to vaccine-mediated protection against SARS-CoV infection in mice (66), and recovery from SARS is accompanied by the development of a neutralizing antibody response in human patients (9, 26, 47). To analyze the impact of SARS S cleavage by TMPRSS2 on antibody-mediated neutralization, we employed sera from mice immunized with soluble S protein. Preincubation of SARS S wild-type (wt) pseudotypes with serum R1LI1, which was generated by immunization of mice with a baculovirus-expressed S protein (21), caused a profound and dose-dependent reduction in viral infectivity (Fig. 2B and raw data in the legend). Strikingly, the reduction was much less pronounced for pseudotypes generated in TMPRSS2-expressing cells, and similar results were obtained with serum R1 (21) although the overall neutralizing activity of this serum was

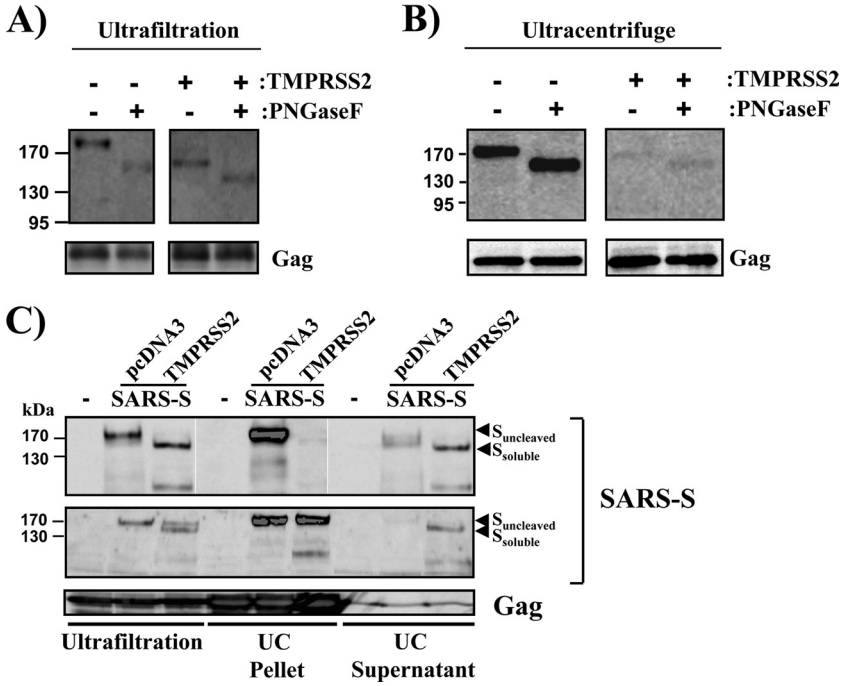

FIG. 3. Cleavage by TMPRSS2 induces SARS S shedding. (A) VLPs were produced in 293T cells in the absence and presence of TMPRSS2, concentrated by ultrafiltration, treated with PNGase F to remove N-linked glycans, and analyzed for SARS S and Gag protein content by Western blotting. Results of a single gel are shown, from which irrelevant lanes were removed. (B) The experiment was carried out as in panel A, but VLPs were additionally concentrated by ultracentrifugation through a 20% sucrose cushion. (C) VLPs were produced as described in panel A and then subjected to ultrafiltration followed by ultracentrifugation. Western blot analysis was employed to determine the effect of these procedures on the concentrations of SARS S and Gag protein in the VLP preparations. Ultrafiltration, VLP preparation subjected to ultrafiltration; UC pellet, VLP preparation subjected to ultrafiltration followed by ultracentrifugation and Western blot analysis of the pellets; UC supernatant, VLP preparation subjected to ultrafiltration followed by ultracentrifugation and Western blot analysis of the supernatants of ultracentrifuge reactions.

lower (Fig. 2B). These results, which were confirmed with two independently generated virus stocks (data not shown), indicate that cleavage by TMPRSS2 reduces SARS S susceptibility to inhibition by neutralizing antibodies.

TMPRSS2 induces SARS S shedding. In order to understand how cleavage of SARS S by TMPRSS2 reduces neutralization sensitivity, we characterized the nature of the cleavage fragments. We first asked if the decreased molecular mass of the 150-kDa cleavage product relative to uncleaved SARS S was indeed due to removal of amino acids or was the result of altered S protein glycosylation. The latter scenario required consideration since coexpression of TMPRSS2 and influenza virus hemagglutinin (HA) not only facilitated HA cleavage but also altered HA glycosylation (4). However, the size difference between uncleaved SARS S and the largest S protein fragment obtained upon TMPRSS2 cleavage remained constant after PNGase F digest (Fig. 3A), which removes all N-linked carbohydrates, indicating that changes in glycan composition did not account for the differential gel mobility of these proteins.

For characterization of S-protein-bearing VLPs, we had so far used VLP preparations concentrated by ultrafiltration, which selectively enriched material in cell culture medium with a molecular mass greater than 50 kDa. We next asked if similar results would be obtained with material concentrated by ultracentrifugation through a 20% sucrose cushion. Under these conditions, mainly particle-associated material is pelleted. Notably, when ultracentrifuge-concentrated VLPs were examined, SARS S produced in TMPRSS2- and control-transfected cells showed identical gel mobilities, independently of PNGase F digest (Fig. 3B). In addition, a marked decrease in signal intensity for SARS S from TMPRSS2-expressing cells compared to SARS S from control cells was observed under these conditions (Fig. 3B).

The results described above were most compatible with the interpretation that at least the largest S protein fragment generated by TMPRSS2 is not virion associated but is shed into the culture supernatants. To further investigate this hypothesis, we concentrated VLP preparations by ultrafiltration and subsequently by ultracentrifugation and determined the effects of these procedures on the presence of uncleaved and cleaved SARS S. As observed before (Fig. 1), SARS S signals of similar intensities were observed upon concentration of VLPs produced in TMPRSS2- and control-transfected cells, and the largest S protein fragment detected in VLPs from TMPRSS2-expressing cells migrated faster than uncleaved SARS S (Fig. 3C, top panel). The differential gel migration remained when VLPs were further subjected to ultracentrifugation, and supernatants were analyzed by Western blotting (Fig. 3C, top panel). However, the signal measured for uncleaved SARS S was markedly reduced compared to that detected for cleaved SARS S (Fig. 3C, top panel), indicating that the former was selectively removed from the supernatants by ultracentrifugation, as expected for virion-associated S protein. Indeed, analysis of pellets revealed a massive concentration of uncleaved

SARS S (Fig. 3C, top panel). In contrast, only a faint signal was obtained for VLPs from TMPRSS2-expressing cells, and the respective S protein migrated identically to uncleaved SARS S (Fig. 3C, top panel). In some experiments incomplete cleavage of SARS S by TMPRSS2 was observed upon analysis of VLPs concentrated by ultrafiltration, with a band corresponding to full-length SARS S still being readily detectable (Fig. 3C, middle panel). When these VLPs were subjected to ultracentrifugation, a prominent signal for uncleaved SARS S was detected in the pellets (Fig. 3C, middle panel), indicating that upon incomplete cleavage of SARS S by TMPRSS2, full-length S protein was incorporated into VLPs. Finally, analysis of the HIV Gag contents of VLP preparations confirmed that VLPs were efficiently pelleted upon ultracentrifugation (Fig. 3C, bottom panel). Collectively, these results suggest that cleavage of SARS S by TMPRSS2 induces SARS S shedding. However, cleavage is incomplete, and a fraction of SARS S produced in TMPRSS2-expressing cells remains uncleaved and is incorporated into particles.

TMPRSS2-dependent SARS S shedding confers resistance against antibody-mediated neutralization. Having demonstrated that TMPRSS2 induces SARS S shedding, we investigated the role of shed SARS S protein in susceptibility of SARS S pseudotypes to inhibition by neutralizing antibodies. For this, we first compared neutralization sensitivity of SARS S pseudotypes generated in TMPRSS2- and control-transfected cells after purification of virions by ultracentrifugation through a 20% sucrose cushion. Under these conditions, virions produced in the presence and absence of TMPRSS2 exhibited comparable neutralization sensitivities (Fig. 4A), indicating that, indeed, a non-particle-associated factor present in virion preparations from TMPRSS2-transfected cells but not from control-transfected cells was responsible for the previously observed neutralization resistance. Western blot analysis confirmed the absence of cleaved SARS S in (ultracentrifuge-concentrated) virions generated in TMPRSS2-expressing cells (Fig. 4B), indicating that the presence of shed SARS S predicts neutralization sensitivity. Finally, our Western blot analysis showed that virion incorporation of uncleaved SARS S was markedly reduced in TMPRSS2-transfected cells relative to control-transfected cells (Fig. 4B), confirming the hypothesis that a fraction of SARS S remains uncleaved and is incorporated into virions in TMPRSS2-expressing cells.

To directly demonstrate that shed SARS S confers neutralization resistance, we purified shed SARS S. For this, we transiently expressed SARS S in the presence and absence of TMPRSS2. Subsequently, the cellular supernatants were concentrated by ultrafiltration and then subjected to ultracentrifugation through a 20% sucrose cushion to remove S protein potentially associated with vesicles released from S protein-transfected cells. The supernatants of the ultracentrifuged samples were collected and analyzed for the presence of S protein by Western blotting (Fig. 4C). As expected, the SARS S cleavage fragments previously observed upon coexpression of TMPRSS2 were concentrated under these conditions (Fig. 4C), confirming that they were shed into the cellular supernatants. In contrast, uncleaved SARS S was absent in samples from TMPRSS2-expressing cells and barely detectable in samples from control-transfected cells (Fig. 4C), demonstrating that uncleaved SARS S is either virion or cell associated, as expected. The material purified under these conditions was then added to SARS S pseudotypes purified by ultracentrifugation, and its effect on neutralization resistance was analyzed. Strikingly, the concentrated supernatants from TMPRSS2-expressing cells (containing shed SARS S) conferred neutralization resistance to SARS S pseudotypes in a dose-dependent manner, while the supernatants from control-transfected cells did not (Fig. 4D), demonstrating that TMPRSS2-dependent shedding of SARS S induces neutralization resistance.

TMPRSS2 cleaves and activates SARS S in *trans*. The results obtained so far indicated that TMPRSS2 cleaves SARS S when both proteins are coexpressed in the same cell. We next examined if TMPRSS2 was also able to cleave SARS S when both proteins were expressed on different cells (*trans*-cleavage), a scenario that mimics contact of infected cells with TMPRSS2-positive cells in the infected host. When cells expressing SARS S were mixed with TMPRSS4-expressing cells or with control-transfected cells, SARS S remained uncleaved (Fig. 5A). In contrast, mixing SARS S- and TMPRSS2-expressing cells resulted in SARS S cleavage, and S protein fragments of the previously observed sizes were detected in the culture supernatants (Fig. 5A). Thus, TMPRSS2 facilitates *trans*-cleavage of SARS S.

In order to investigate potential consequences of *trans*-cleavage for SARS S activity, we asked if expression of TMPRSS2 on target cells impacts the efficiency of SARS S-driven cell-to-cell fusion. For this, we measured fusion of 293T effector cells transfected to express SARS S with 293T target cells transfected to express ACE2 or TMPRSS2, employing a previously described cell-cell fusion assay (28). In addition, target cells expressing the TMPRSS2-related proteases TMPRSS4, TMPRSS3, TMPRSS6, and hepsin were tested; none of the latter three was previously associated with activation of viral glycoproteins. Effector and target cells transfected with empty vector served as controls. SARS S-driven fusion with cells transfected with empty plasmid was inefficient (Fig. 5B), as expected, since 293T cells express only small amounts of endogenous ACE2, which are insufficient to support robust cell-cell fusion (36). Similarly, no appreciable membrane fusion activity was detected when effector cells were transfected with empty plasmid instead of plasmid encoding SARS S (Fig. 5B). In contrast, trypsin treatment of effector and target cell mixtures or overexpression of ACE2 on target cells allowed efficient SARS S-driven cell-cell fusion (Fig. 5B), indicating that proteolytic activation of SARS S is required for SARS S-driven cell-cell fusion only when receptor expression is limiting. Expression of TMPRSS2 on target cells also allowed efficient SARS S-dependent cell-cell fusion, while expression of TMPRSS3, TMPRSS6, and hepsin did not (Fig. 5B), indicating that *trans*-cleavage by TMPRSS2 can activate SARS S for cell-cell fusion. Unexpectedly, expression of TMPRSS4 on target cells also activated SARS S for membrane fusion (Fig. 5B). TMPRSS4 failed to cleave SARS S (Fig. 1 and 5A), and the molecular mechanism underlying SARS S activation by TMPRSS4 is at present unclear.

We then asked if the augmentation of SARS S-driven cell-cell fusion by TMPRSS2 (Fig. 5B) is reflected by increased syncytium formation in TMPRSS2-positive cells infected with replication-competent SARS-CoV. To this end, we examined the impact of protease expression on syncytium formation in

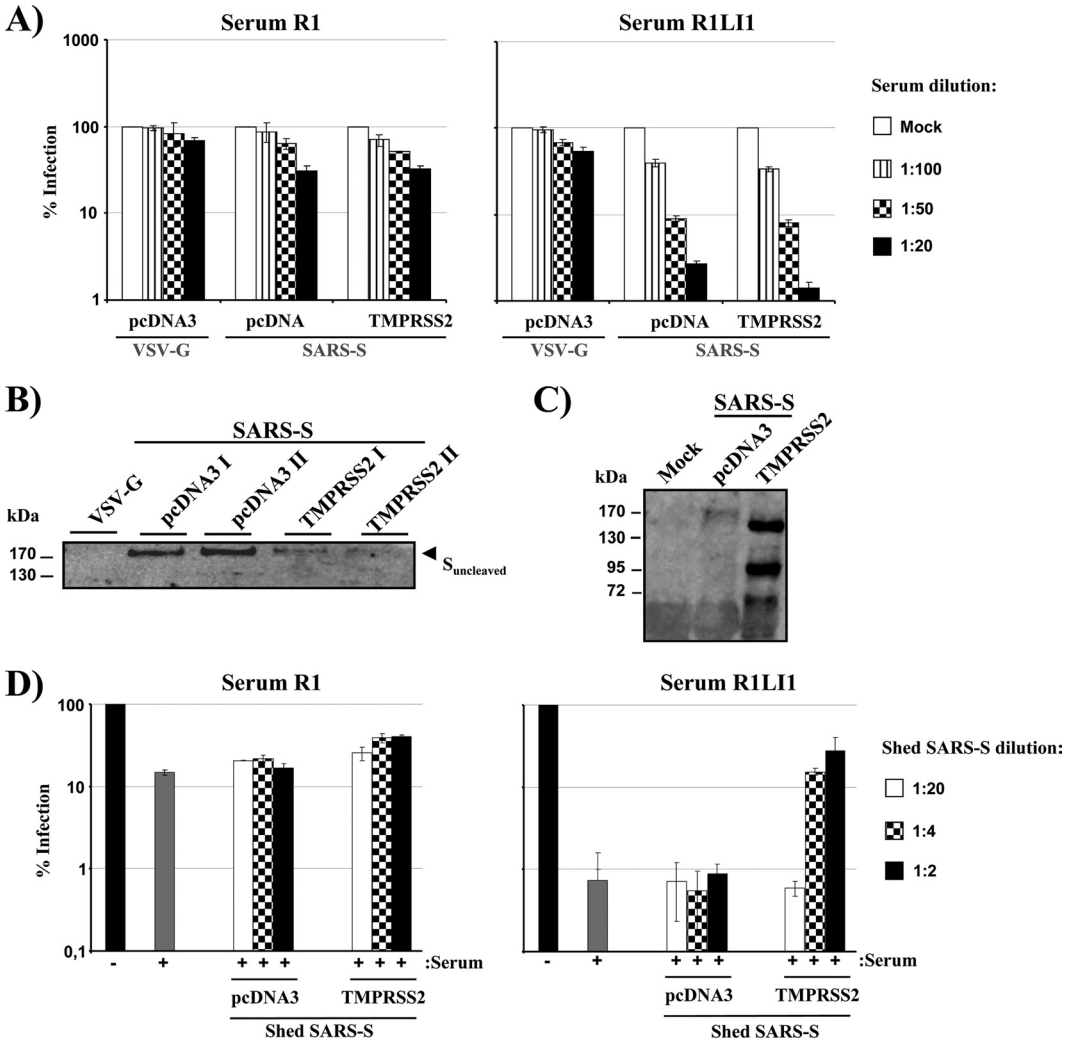

FIG. 4. Shedding of SARS S by TMPRSS2 confers neutralization resistance. (A) The pseudoparticles indicated were produced in 293T cells in the presence or absence of TMPRSS2, concentrated by ultracentrifugation through a 20% sucrose cushion, preincubated with the indicated dilutions of the sera R1 and R1LI1, and then used for triplicate infections of 293T-ACE2 cells. Luciferase activities in cell lysates were determined after 72 h, and activities measured in the absence of serum were set as 100%. The results of a representative experiment are shown; error bars indicate standard deviations. The results were confirmed in two independent experiments. In the absence of serum, the following luciferase counts were measured: VSV-G, 509,961 ± 37,823 cps; SARS S plus pcDNA3, 497,873 ± 52,794 cps; SARS S plus TMPRSS2, 608,600 ± 97,835 cps. (B) The concentrated pseudotypes described in panel A were analyzed by Western blotting for the presence of SARS S (employing an S1-specific rabbit serum). (C) 293T cells were transiently cotransfected with expression plasmids for SARS S and TMPRSS2 or cotransfected with SARS S plasmid and empty vector (pcDNA3), and culture supernatants were harvested at 48 h after transfection. Subsequently, the supernatants were concentrated by ultrafiltration followed by ultracentrifugation through a 20% sucrose cushion. The presence of soluble SARS S protein in the supernatants of ultracentrifuged samples was analyzed by immunoblotting, as described in panel A. (D) Pseudoparticles bearing SARS S and purified by ultracentrifugation through a sucrose cushion were preincubated with the indicated dilutions of supernatants described in panel C and a 1:50 dilution of the sera R1 and R1LI1 for 60 min before addition to target cells (pcDNA3, supernatants from cells cotransfected with SARS-S and empty plasmid; TMPRSS2, supernatants from cells cotransfected with TMPRSS2 and SARS S expression plasmids). Luciferase activities in cell lysates were determined after 72 h. The results ± standard deviations of a representative experiment carried out in triplicate are shown; activities measured in the absence of serum, 1,307,409 ± 328118 cps, were set as 100%. The results were confirmed in two separate experiments.

Vero E6 cells, which are commonly used to analyze SARS-CoV spread. Large syncytia were frequently detected in TMPRSS2-expressing Vero E6 cells infected with SARS-CoV (Frankfurt strain 1), while syncytia in TMPRSS4-expressing cells and in control-transfected cells were largely absent (Fig. 5C). These results suggest that TMPRSS2 but not TMPRSS4 is able to activate SARS-S in the context of surrogate systems and in the context of authentic SARS-CoV.

TMPRSS2 on target cells allows efficient SARS S-driven virus-cell fusion in the presence of a lysosomotropic agent and a cathepsin inhibitor. The SARS S-driven virus-cell fusion depends on endosomal low pH and the activity of the pH-dependent endosomal protease cathepsin L (53, 55). Consequently, infectious entry can be inhibited by lysosomotropic agents like ammonium chloride (NH_4Cl), which elevates the endosomal pH, and by cathepsin L inhibitors like MDL 28170

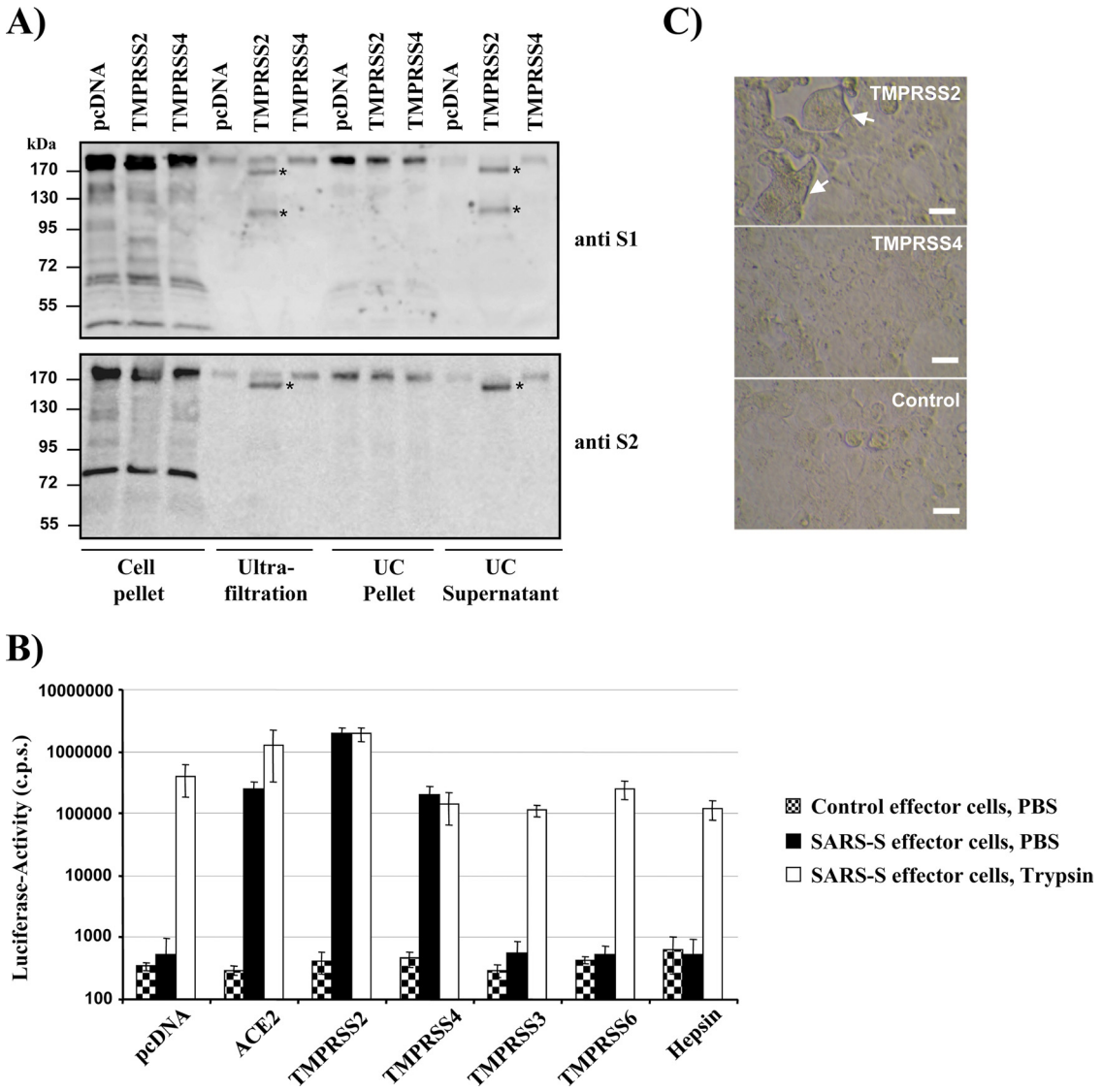

FIG. 5. TMPRSS2 cleaves SARS S in *trans* and activates SARS S for cell-cell fusion. (A) Effector cells were transfected with SARS S expression plasmid and mixed with target cells transfected with empty plasmid (pcDNA) or plasmids encoding TMPRSS2 or TMPRSS4. Lysates and supernatants of these cell mixtures were analyzed for SARS S cleavage by Western blotting, employing sera directed against the S1 and the S2 portions of SARS S for detection. Before analysis by Western blotting, supernatants were concentrated by ultrafiltration and ultracentrifugation. Cell pellet, lysates of transfected cells analyzed by Western blotting; Ultrafiltration, culture supernatants subjected to ultrafiltration followed by Western blot analysis; UC pellet, culture supernatants subjected to ultrafiltration followed by ultracentrifugation and Western blot analysis of the pellets; UC supernatant, culture supernatants subjected to ultrafiltration followed by ultracentrifugation and Western blot analysis of the supernatants of ultracentrifuge reactions. (B) Effector cells cotransfected with pGAL4-VP16 expression plasmid and either empty plasmid or SARS S expression plasmid were mixed with target cells cotransfected with the indicated plasmids and a plasmid encoding luciferase under the control of a promoter with multiple GAL4 binding sites. The cell mixtures were then treated with either PBS or trypsin, and the luciferase activities in cell lysates were quantified at 48 h after cell mixing. The results of a representative experiment performed in triplicates are shown; error bars indicate standard deviations. Similar results were observed in two independent experiments. (C) Vero E6 cells transfected with TMPRSS2 or TMPRSS4 expression plasmid or empty vector (pcDNA) were infected with SARS-CoV (Frankfurt strain 1) at an MOI of 0.1. At 29 h postinfection the cells were fixed and analyzed by microscopy. Bar, 20 μm. Arrows indicate syncytia. Similar results were obtained in an independent experiment.

(53, 55). In the light of the efficient cleavage and activation of SARS S by TMPRSS2, we asked if activation of virion-associated SARS S by TMPRSS2 might allow SARS S-driven infectious entry into cells treated with NH_4Cl or MDL 28170. Infectious entry of SARS S pseudotypes into control transfected 293T-hACE2 cells was efficiently inhibited by both NH_4Cl and MDL 28170, and inhibition was unaffected by expression of TMPRSS4 on target cells (Fig. 6A). In contrast, expression of TMPRSS2 on target cells markedly reduced inhibition of SARS S-driven entry by NH_4Cl and MDL 28170 (Fig. 6A). Importantly, similar results were obtained when cellular entry of authentic SARS-CoV was examined; expression of TMPRSS2 did not modulate entry into mock-treated cells, as judged by the presence of N gene mRNA in cell lysates, but allowed efficient viral entry into cells treated with MDL 28170 (Fig. 6B). In contrast, the expression of TMPRSS4 had no

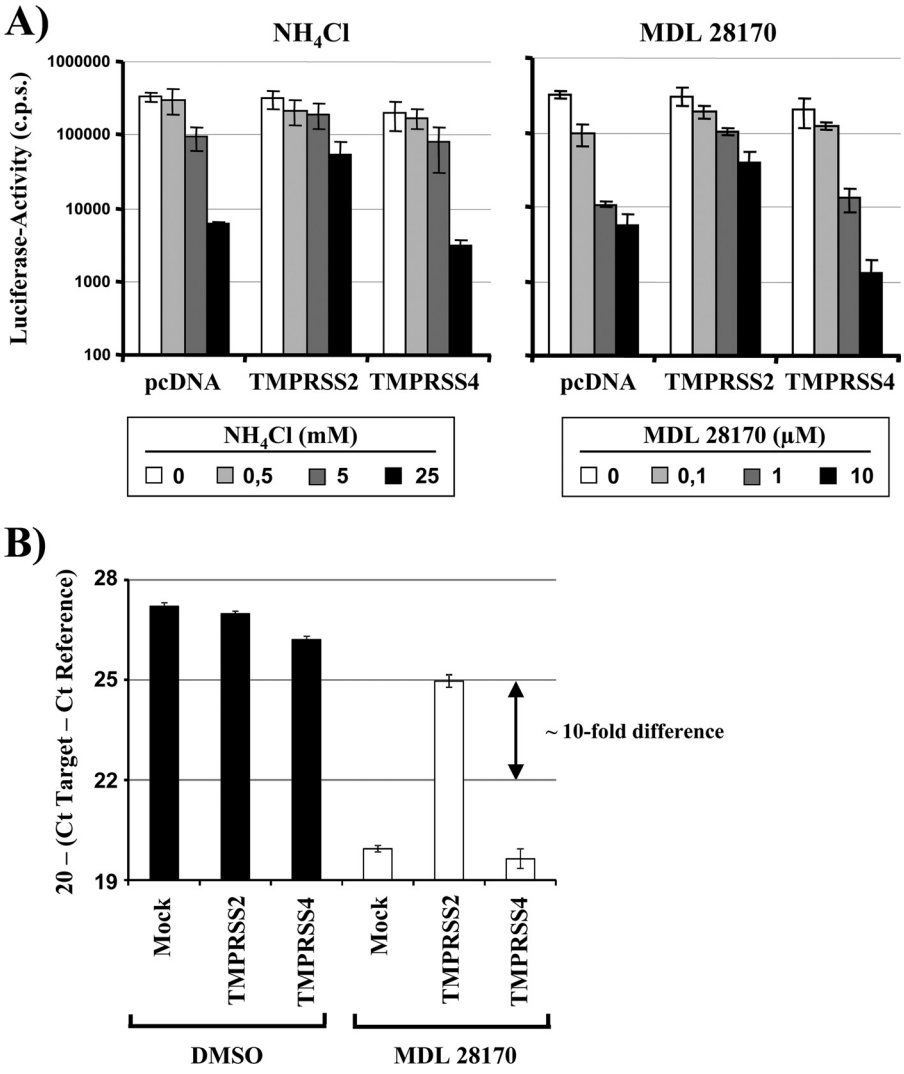

FIG. 6. Expression of TMPRSS2 on target cells reduces the requirement for acidic pH and cathepsin activity for SARS S-driven infectious entry. (A) The indicated proteases were expressed in 293T-hACE2 cells, and the cells were pretreated with medium containing the indicated concentrations of NH_4Cl and MDL 28170. Subsequently, the cells were infected with pseudotypes bearing SARS S in the presence of inhibitor. The infection medium was replaced by fresh medium without inhibitor at 16 h postinfection, and the luciferase activities in cell lysates were analyzed at 72 h postinfection. The results of representative experiments performed in triplicates are shown; error bars indicate standard deviations. Similar results were obtained in two independent experiments. (B) The indicated proteases were expressed in 293T-hACE2 cells, and the cells were treated with the cathepsin inhibitor MDL 28170 before infection with SARS-CoV (Frankfurt strain 1) at an MOI of 0.1. At 5 h postinfection the cells were washed with PBS and lysed, and total RNA was extracted. SARS-CoV entry was analyzed by real-time RT-PCR specific for the N gene mRNA. Average C_T values of a single experiment performed in triplicates were normalized by subtracting the respective C_T values for TATA-box binding protein (reference gene). For clarity, values were subtracted by a fixed number (20). A C_T difference of 3 correlated approximately with a 10-fold increase in transcripts as determined by a dilution series of both targets. Similar results were obtained in an independent experiment.

effect (Fig. 6B). These results indicate that activation of virion-associated SARS S by TMPRSS2 can render low pH and cathepsin L activity dispensable for virus-cell fusion.

TMPRSS2 and ACE2 are coexpressed by type II pneumocytes. In order to address whether SARS S could be cleaved by TMPRSS2 in the lung of SARS-CoV-infected patients, we first determined expression of mRNA for TMPRSS2 in human tissues. mRNA was low or absent in brain and heart tissue but was readily detected in tissue samples obtained from pancreas, kidney, and lung (Fig. 7A). We then determined if the presence of TMPRSS2 mRNA in human lung was reflected by expression of TMPRSS2 protein, and we analyzed if the protein expression patterns of TMPRSS2 and ACE2 were overlapping. For this, human lung epithelium was analyzed by immunohistochemistry, employing a monoclonal antibody against TMPRSS2 (41) and a polyclonal serum directed against ACE2. Immunostaining for TMPRSS2 and ACE2 demonstrated strong positive staining of type II pneumocytes and alveolar macrophages, while type I pneumocytes were negative (Fig. 7B). Incubation of tissues with control antibodies did not result in significant staining. Thus, TMPRSS2 and ACE2 are coexpressed by type II pneumocytes, which consti-

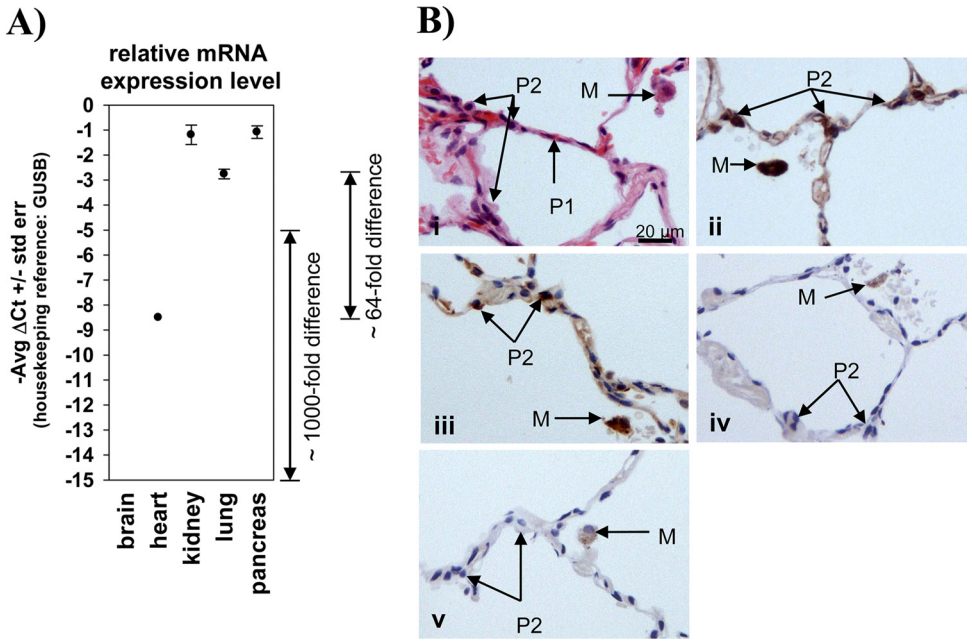

FIG. 7. Coexpression of ACE2 and TMPRSS2 on type II pneumocytes. (A) The amount of *Tmprss2* transcript in the indicated organs was quantified by PCR, employing GUSB as a housekeeping reference. The averages of three independent experiments are shown; error bars indicate standard deviations (std err). No specific signal was measured for brain in three out of three experiments. A specific signal was measured for heart in one out of three independent experiments. (B, i) Hematoxylin-and-eosin-stained section of normal lung showing several alveolar spaces, in which alveolar macrophages (M), type I pneumocytes (P1), and type II pneumocytes (P2) are labeled. Scale bar, 20 μm. (ii) Serial section of frame i immunostained for TMPRSS2 using the peroxidase technique (brown) shows strong positive staining in type II pneumocytes and alveolar macrophages. (iii) Serial section of frame ii immunostained for ACE-2 shows strong positive staining in type II pneumocytes and alveolar macrophages. (iv) Serial section of frame iii immunostained with an irrelevant mouse primary antibody (melan-A), as a negative control for frame ii, shows no immunostaining. Alveolar macrophages show a faint brown tint, due to the presence of carbon, but not the strong brown staining of macrophages seen in frame ii. (v) Serial section of frame iv immunostained using goat polyclonal serum as a primary antibody, as a negative control for frame iii. Alveolar macrophages show a faint brown tint, due to the presence of carbon, but not the strong brown staining of macrophages seen in frames ii and iii.

tute major targets for SARS-CoV (20, 45, 58), indicating that SARS S could be processed by TMPRSS2 in the lung of infected humans.

DISCUSSION

Processing of viral glycoproteins by host cell proteases can have several consequences. Cleavage can increase or can be essential for viral infectivity (3, 10, 15, 17, 30). In addition, cleavage can result in glycoprotein shedding (12), and the shed proteins can act as antibody decoys (12) or can modulate cellular functions by binding to host cell receptors. We show that the SARS S protein is cleaved by TMPRSS2 and that cleavage has different consequences, depending on the location of TMPRSS2. If TMPRSS2 is coexpressed with SARS S in the same cell, cleavage results in SARS S shedding into the supernatants, where the S protein fragments function as antibody decoys. If TMPRSS2 is expressed on viral target cells, it can activate SARS S for virus-cell and cell-cell fusion. Finally, TMPRSS2 was found to be coexpressed with the SARS-CoV receptor ACE2 on type II pneumocytes, which are major viral target cells (20, 45, 58), indicating that SARS S cleavage by TMPRSS2 could modulate viral spread in the infected host.

Simmons and colleagues demonstrated that inhibition of cathepsin activity blocks infectious cellular entry of SARS-CoV (53), indicating that cathepsins proteolytically activate SARS S upon viral uptake into target cell endosomes. In contrast, the efficiency and functional relevance of SARS S processing in productively infected cells are less clear (3, 15, 55, 63, 64, 67). In the majority of studies, one or two prominent bands (due to differential glycosylation) representative of full-length SARS S have been detected upon analysis of SARS S expression in transiently transfected or infected cells. Exceptions are the findings by Wu and colleagues, who reported efficient cleavage of SARS S in infected Vero E6 cells (63), and Du and colleagues, who provided evidence of SARS-S cleavage by factor Xa (13). It has also been suggested that furin cleaves SARS S and thereby moderately augments viral infectivity (3, 15). However, the cleavage efficiency seems to be low. Similarly, a recent study reported cleavage of recombinant trimeric SARS S by trypsin, plasmin, and TMPRSS11a; cleavage was not demonstrated in the context of cellular or virion-associated SARS S, however, and cleavage was associated with only a minor increase in infectivity of SARS S pseudotypes (30). Collectively, there is little evidence that SARS S is efficiently processed by proteases in productively infected cells. However, SARS S processing by pulmonary proteases has rarely been examined.

We along with others have previously shown that the type II transmembrane serine proteases TMPRSS2 and TMPRSS4 proteolytically activate human influenza viruses (6, 8), and it is

conceivable that these proteases might support viral spread in and between infected individuals (5). When we assessed the impact of TMPRSS2 and TMPRSS4 expression on the proteolytic processing of SARS S, cleavage of SARS S into several fragments was observed upon coexpression of TMPRSS2 but not TMPRSS4. Thus, SARS S, like influenza virus HA (6, 8) and human metapneumovirus fusion protein (51), is cleaved by TMPRSS2. However, in contrast to these other proteins, which are processed by TMPRSS2 at a single site, SARS S is cleaved at multiple motifs, indicating that the functional consequences of cleavage might be different.

A previous study indicated that the introduction of an artificial cleavage site into SARS S can allow cathepsin-independent infection (61). Similar results were not observed with viruses produced in TMPRSS2-expressing cells, with minor differences in sensitivity to high doses of cathepsin inhibitors reflecting variability inherent to the experimental system rather than biologically meaningful differences. However, pseudotypes produced in the presence of TMPRSS2 were largely resistant to neutralization by two different mouse sera obtained by immunization of animals with recombinant SARS S (21). Although differences in the neutralization efficiency of SARS S pseudotypes and SARS-CoV might exist, this finding could have important implications for SARS-CoV spread in the infected host. Thus, the humoral immune response critically contributes to immune control of SARS-CoV infection (9, 26, 47, 66), and a delayed or diminished control of SARS-CoV by antibodies due to TMPRSS2 might contribute to disease progression. Such a scenario raises the question of how cleavage by TMPRSS2 modulates SARS S neutralization sensitivity.

To understand the mechanisms underlying neutralization resistance of SARS S pseudotypes generated in TMPRSS2-expressing cells, we characterized the SARS S cleavage products. Analysis by PNGase F digest showed that size differences between uncleaved and TMPRSS2 cleaved SARS S were not due to differential glycosylation, which has been observed for influenza virus HA generated in TMPRSS2 relative to TMPRSS4-transfected and control-transfected cells (4). In addition, analysis of cleavage products by ultracentrifugation revealed that SARS S fragments produced by TMPRSS2 did not pellet in a 20% sucrose cushion, indicating that they were not virion associated. It must be noted, however, that cleavage of SARS S by TMPRSS2 was frequently incomplete, with some uncleaved SARS S or potential cleavage intermediates still being detectable by Western blotting. As a consequence, pseudotypes generated in the presence of TMPRSS2 retained substantial infectivity and were largely protected against antibody-mediated neutralization, due to the presence of shed SARS S in the virion preparations, as demonstrated by the findings that removal of shed SARS S from virus preparations ablated neutralization resistance while addition of shed SARS S conferred neutralization resistance.

The SARS S sequence motifs cleaved by TMPRSS2 are at present unknown. Trypsin treatment of SARS S produced single S1 and S2 fragments, as expected from published data (2, 43), and similar fragments were not, or only inefficiently, produced by TMPRSS2, indicating that TMPRSS2 and trypsin recognize different motifs in SARS S. Analysis of SARS S cleavage products with antiserum directed against defined portions of SARS S revealed that the largest cleavage fragment (150 kDa) was most likely produced by a cleavage event occurring between amino acids 1152 and 1200 (data not shown). If so, the 150-kDa fragment contained the conserved receptor binding domain (RBD) in SARS S, amino acids 318 to 510 (1, 35, 62, 64), which is a major target for neutralizing antibodies (22–24), and an antibody decoy function of this fragment would thus be conceivable.

There is evidence that type II transmembrane serine proteases can activate the influenza virus hemagglutinin in productively infected cells and upon binding and uptake of virions into uninfected cells (7). This finding prompted us to examine if expression of TMPRSS2 on target cells allowed SARS S cleavage. SARS S cleavage products in cell lysates and cellular supernatants were, indeed, readily detected when SARS S-expressing cells were mixed with TMPRSS2-expressing cells. No such effect was observed with TMPRSS4-positive cells or control transfected cells, indicating that cleavage was specific. However, differences in the relative amounts of cleavage products were noted on comparison of *trans*- and *cis*-cleavage of SARS S by TMPRSS2. Thus, the SARS S processing products of 45 kDa und 55 kDA observed upon *cis*-cleavage were usually not detected upon *trans*-cleavage, suggesting that TMPRSS2 might recognize the cleavage sites in SARS S with different efficiencies and that only high-affinity sites might be cleaved in *trans*.

Expression of SARS S on effector cells can allow fusion with receptor-positive target cells, resulting in the formation of syncytia (36, 55, 64), which are also detected in infected patients (32, 46). Addition of trypsin to mixtures of SARS S effector cells and ACE2-positive target cells is believed to be required for efficient cell-cell fusion (55, 64), and our results show that expression of the trypsin-like protease TMPRSS2 on target cells can functionally replace exogenous trypsin. Overexpression of ACE2 on 293T target cells, which produce small amounts of endogenous ACE2, also allowed efficient SARS S-driven cell-cell fusion, indicating that proteolytic activation of SARS S is required only for cell-cell fusion when receptor levels are limiting. Unexpectedly, expression of TMPRSS4 on target cells promoted SARS S-driven cell-cell fusion with an efficiency similar to that of TMPRSS2 but failed to produce detectable levels of SARS S cleavage in the *trans* and *cis* settings. Although the molecular mechanism underlying SARS S activation by TMPRSS4 is at present unclear, one can speculate that low levels of cleavage might be responsible. Importantly, TMPRSS2 but not TMPRSS4 promoted formation of syncytia in SARS-CoV-infected cell cultures, indicating that only TMPRSS2 can activate SARS-CoV for spread in host cells.

Infectious SARS-CoV entry into target cells depends on the activity of the pH-dependent endosomal cysteine protease cathepsin L and to a lesser degree on the related enzyme cathepsin B (53). Both proteases depend on low pH for their activity, and SARS-CoV entry can therefore be blocked by lysosomotropic agents (which elevate endosomal pH) and by cathepsin inhibitors (26, 53, 55, 65). Previous studies indicate that the requirement for low pH and cathepsin activity for SARS S-driven virus-cell fusion can be bypassed by treatment of cell-bound virions with trypsin (55) or insertion of an artificial cleavage site into SARS S (61). Similarly to these findings, expression of TMPRSS2 was sufficient to allow robust

entry of SARS S pseudotypes into cells treated with NH_4Cl and the cathepsin L inhibitor MDL 28170, a compound that was previously shown to inhibit SARS S infectious entry (53); this observation was confirmed with authentic SARS-CoV. In contrast, TMPRSS4 was inactive in this setting, suggesting that activation of SARS S by this protease might occur only upon high-level expression of SARS S and protease and/or upon interaction of large surfaces bearing these proteins, hallmarks of the cell-cell fusion assay. In sum, TMPRSS2 but not TMPRSS4 allows SARS-CoV to bypass a block otherwise imposed by cathepsin inhibitors. This observation, in conjunction with our finding that type II pneumocytes, which are major SARS-CoV target cells, coexpress TMPRSS2 and ACE2, suggests that cathepsin inhibitors might not be able to efficiently suppress viral spread in infected patients.

We report that TMPRSS2 can cleave SARS S in *cis* and in *trans*, with different consequences for SARS S function. It is noteworthy that TMPRSS2 is believed to cleave its substrates at the cell surface and/or in intracellular vesicles (7, 41) probably located close to the cell surface. However, a major fraction of SARS S is retained in the ERGIC (44, 56, 59) in infected cells and might thus be inaccessible to TMPRSS2 for *cis*-cleavage. Indeed, a recent study by Matsuyama and colleagues, which was published while the present manuscript was in revision, indicated that TMPRSS2 might not cleave SARS S in *cis* in infected cell lines (42). Nevertheless, two reports demonstrated that some SARS S is transported to the surface of infected cells (48, 59), where *cis*- and *trans*-cleavage by TMPRSS2 could occur, and it is possible that SARS S is shed by type II pneumocytes, which might express higher levels of TMPRSS2 than the cell lines examined so far. While *cis*-cleavage of SARS S awaits further investigation, our present results unambiguously demonstrate that SARS S incorporated into both lentiviral pseudotypes and authentic SARS-CoV particles is activated by TMPRSS2 during host cell entry. Therefore, fully activated virions might be delivered to the endosomal compartment of type II pneumocytes and potentially other host cells, which would compromise the effectiveness of cathepsin inhibitors as antiviral agents, in agreement with recent findings (42, 52). Clearly, the role of TMPRSS2 in SARS-CoV spread and pathogenesis warrants further investigation, and *Tmprss2* knockout mice, which do not display an obvious phenotype (31), might be a useful tool for these studies.

ACKNOWLEDGMENTS

We thank T. F. Schulz for support, P. Nelson and J. Lucas for the kind gift of P5H9 antibody and K. Korn for the p24 enzyme-linked immunosorbent assay.

This work was supported by BMBF (grant 01KI 0703), the Center for Infection Biology (I.S.), and the Ph.D. program Molecular Medicine (T.S.T.).

REFERENCES

1. **Babcock, G. J., D. J. Esshaki, W. D. Thomas, Jr., and D. M. Ambrosino.** 2004. Amino acids 270 to 510 of the severe acute respiratory syndrome coronavirus spike protein are required for interaction with receptor. J. Virol. **78:**4552–4560.
2. **Belouzard, S., V. C. Chu, and G. R. Whittaker.** 2009. Activation of the SARS coronavirus spike protein via sequential proteolytic cleavage at two distinct sites. Proc. Natl. Acad. Sci. U. S. A. **106:**5871–5876.
3. **Bergeron, E., et al.** 2005. Implication of proprotein convertases in the processing and spread of severe acute respiratory syndrome coronavirus. Biochem. Biophys. Res. Commun. **326:**554–563.
4. **Bertram, S., et al.** 2010. TMPRSS2 and TMPRSS4 facilitate trypsin-independent spread of influenza virus in Caco-2 cells. J. Virol. **84:**10016–10025.
5. **Bertram, S., I. Glowacka, I. Steffen, A. Kuhl, and S. Pöhlmann.** 2010. Novel insights into proteolytic cleavage of influenza virus hemagglutinin. Rev. Med. Virol. **20:**298–310.
6. **Bottcher, E., et al.** 2006. Proteolytic activation of influenza viruses by serine proteases TMPRSS2 and HAT from human airway epithelium. J. Virol. **80:**9896–9898.
7. **Bottcher-Friebertshauser, E., et al.** 2010. Cleavage of influenza virus hemagglutinin by airway proteases TMPRSS2 and HAT differs in subcellular localization and susceptibility to protease inhibitors. J. Virol. **84:**5605–5614.
8. **Chaipan, C., et al.** 2009. Proteolytic activation of the 1918 influenza virus hemagglutinin. J. Virol. **83:**3200–3211.
9. **Chen, X., et al.** 2004. Serology of severe acute respiratory syndrome: implications for surveillance and outcome. J. Infect. Dis. **189:**1158–1163.
10. **Choi, S. Y., S. Bertram, I. Glowacka, Y. W. Park, and S. Pöhlmann.** 2009. Type II transmembrane serine proteases in cancer and viral infections. Trends Mol. Med. **15:**303–312.
11. **Connor, R. I., B. K. Chen, S. Choe, and N. R. Landau.** 1995. Vpr is required for efficient replication of human immunodeficiency virus type-1 in mononuclear phagocytes. Virology **206:**935–944.
12. **Dolnik, O., et al.** 2004. Ectodomain shedding of the glycoprotein GP of Ebola virus. EMBO J. **23:**2175–2184.
13. **Du, L., et al.** 2007. Cleavage of spike protein of SARS coronavirus by protease factor Xa is associated with viral infectivity. Biochem. Biophys. Res. Commun. **359:**174–179.
14. **Eckert, D. M., and P. S. Kim.** 2001. Mechanisms of viral membrane fusion and its inhibition. Annu. Rev. Biochem. **70:**777–810.
15. **Follis, K. E., J. York, and J. H. Nunberg.** 2006. Furin cleavage of the SARS coronavirus spike glycoprotein enhances cell-cell fusion but does not affect virion entry. Virology **350:**358–369.
16. **Gao, F., et al.** 2003. Codon usage optimization of HIV type 1 subtype C *gag*, *pol*, *env*, and *nef* genes: in vitro expression and immune responses in DNA-vaccinated mice. AIDS Res. Hum. Retroviruses **19:**817–823.
17. **Garten, W., and H. D. Klenk.** 1999. Understanding influenza virus pathogenicity. Trends Microbiol. **7:**99–100.
18. **Glowacka, I., et al.** 2010. Differential downregulation of ACE2 by the spike proteins of severe acute respiratory syndrome coronavirus and human coronavirus NL63. J. Virol. **84:**1198–1205.
19. **Guan, Y., et al.** 2003. Isolation and characterization of viruses related to the SARS coronavirus from animals in southern China. Science **302:**276–278.
20. **Hamming, I., et al.** 2004. Tissue distribution of ACE2 protein, the functional receptor for SARS coronavirus. A first step in understanding SARS pathogenesis. J. Pathol. **203:**631–637.
21. **He, Y., J. Li, S. Heck, S. Lustigman, and S. Jiang.** 2006. Antigenic and immunogenic characterization of recombinant baculovirus-expressed severe acute respiratory syndrome coronavirus spike protein: implication for vaccine design. J. Virol. **80:**5757–5767.
22. **He, Y., H. Lu, P. Siddiqui, Y. Zhou, and S. Jiang.** 2005. Receptor-binding domain of severe acute respiratory syndrome coronavirus spike protein contains multiple conformation-dependent epitopes that induce highly potent neutralizing antibodies. J. Immunol. **174:**4908–4915.
23. **He, Y., et al.** 2004. Receptor-binding domain of SARS-CoV spike protein induces highly potent neutralizing antibodies: implication for developing subunit vaccine. Biochem. Biophys. Res. Commun. **324:**773–781.
24. **He, Y., et al.** 2004. Identification of immunodominant sites on the spike protein of severe acute respiratory syndrome (SARS) coronavirus: implication for developing SARS diagnostics and vaccines. J. Immunol. **173:**4050–4057.
25. **Hofmann, H., et al.** 2004. Susceptibility to SARS coronavirus S protein-driven infection correlates with expression of angiotensin converting enzyme 2 and infection can be blocked by soluble receptor. Biochem. Biophys. Res. Commun. **319:**1216–1221.
26. **Hofmann, H., et al.** 2004. S protein of severe acute respiratory syndrome-associated coronavirus mediates entry into hepatoma cell lines and is targeted by neutralizing antibodies in infected patients. J. Virol. **78:**6134–6142.
27. **Hofmann, H., and S. Pöhlmann.** 2004. Cellular entry of the SARS coronavirus. Trends Microbiol. **12:**466–472.
28. **Hofmann, H., et al.** 2006. Highly conserved regions within the spike proteins of human coronaviruses 229E and NL63 determine recognition of their respective cellular receptors. J. Virol. **80:**8639–8652.
29. **Jung, H., et al.** 2008. TMPRSS4 promotes invasion, migration and metastasis of human tumor cells by facilitating an epithelial-mesenchymal transition. Oncogene **27:**2635–2647.
30. **Kam, Y. W., et al.** 2009. Cleavage of the SARS coronavirus spike glycoprotein by airway proteases enhances virus entry into human bronchial epithelial cells in vitro. PLoS One **4:**e7870.
31. **Kim, T. S., C. Heinlein, R. C. Hackman, and P. S. Nelson.** 2006. Phenotypic analysis of mice lacking the Tmprss2-encoded protease. Mol. Cell. Biol. **26:**965–975.
32. **Kuiken, T., et al.** 2003. Newly discovered coronavirus as the primary cause of severe acute respiratory syndrome. Lancet **362:**263–270.

33. **Lau, S. K., et al.** 2005. Severe acute respiratory syndrome coronavirus-like virus in Chinese horseshoe bats. Proc. Natl. Acad. Sci. U. S. A. **102:**14040–14045.
34. **Li, F., et al.** 2006. Conformational states of the severe acute respiratory syndrome coronavirus spike protein ectodomain. J. Virol. **80:**6794–6800.
35. **Li, F., W. Li, M. Farzan, and S. C. Harrison.** 2005. Structure of SARS coronavirus spike receptor-binding domain complexed with receptor. Science **309:**1864–1868.
36. **Li, W., et al.** 2003. Angiotensin-converting enzyme 2 is a functional receptor for the SARS coronavirus. Nature **426:**450–454.
37. **Li, W., et al.** 2005. Bats are natural reservoirs of SARS-like coronaviruses. Science **310:**676–679.
38. **Li, W., et al.** 2006. Animal origins of the severe acute respiratory syndrome coronavirus: insight from ACE2-S-protein interactions. J. Virol. **80:**4211–4219.
39. **Li, W., et al.** 2005. Receptor and viral determinants of SARS-coronavirus adaptation to human ACE2. EMBO J. **24:**1634–1643.
40. **Lubisch, W., H. P. Hofmann, H. J. Treiber, and A. Moller.** 2000. Synthesis and biological evaluation of novel piperidine carboxamide derived calpain inhibitors. Bioorg. Med. Chem. Lett. **10:**2187–2191.
41. **Lucas, J. M., et al.** 2008. The androgen-regulated type II serine protease TMPRSS2 is differentially expressed and mislocalized in prostate adenocarcinoma. J. Pathol. **215:**118–125.
42. **Matsuyama, S., et al.** 2010. Efficient activation of SARS coronavirus spike protein by the transmembrane protease, TMPRSS2. J. Virol. **84:**12658–12664.
43. **Matsuyama, S., M. Ujike, S. Morikawa, M. Tashiro, and F. Taguchi.** 2005. Protease-mediated enhancement of severe acute respiratory syndrome coronavirus infection. Proc. Natl. Acad. Sci. U. S. A. **102:**12543–12547.
44. **McBride, C. E., J. Li, and C. E. Machamer.** 2007. The cytoplasmic tail of the severe acute respiratory syndrome coronavirus spike protein contains a novel endoplasmic reticulum retrieval signal that binds COPI and promotes interaction with membrane protein. J. Virol. **81:**2418–2428.
45. **Mossel, E. C., et al.** 2008. SARS-CoV replicates in primary human alveolar type II cell cultures but not in type I-like cells. Virology **372:**127–135.
46. **Nicholls, J. M., et al.** 2003. Lung pathology of fatal severe acute respiratory syndrome. Lancet **361:**1773–1778.
47. **Nie, Y., et al.** 2004. Highly infectious SARS-CoV pseudotyped virus reveals the cell tropism and its correlation with receptor expression. Biochem. Biophys. Res. Commun. **321:**994–1000.
48. **Ohnishi, K., et al.** 2005. Immunological detection of severe acute respiratory syndrome coronavirus by monoclonal antibodies. Jpn. J. Infect. Dis. **58:**88–94.
49. **Peiris, J. S., Y. Guan, and K. Y. Yuen.** 2004. Severe acute respiratory syndrome. Nat. Med. **10:**S88–S97.
50. **Radonic, A., et al.** 2004. Guideline to reference gene selection for quantitative real-time PCR. Biochem. Biophys. Res. Commun. **313:**856–862.
51. **Shirogane, Y., et al.** 2008. Efficient multiplication of human metapneumovirus in Vero cells expressing the transmembrane serine protease TMPRSS2. J. Virol. **82:**8942–8946.
52. **Shulla, A., et al.** 2011. A transmembrane serine protease is linked to the severe acute respiratory syndrome coronavirus receptor and activates virus entry. J. Virol. **85:**873–882.
53. **Simmons, G., et al.** 2005. Inhibitors of cathepsin L prevent severe acute respiratory syndrome coronavirus entry. Proc. Natl. Acad. Sci. U. S. A. **102:**11876–11881.
54. **Simmons, G., et al.** 2003. DC-SIGN and DC-SIGNR bind Ebola glycoproteins and enhance infection of macrophages and endothelial cells. Virology **305:**115–123.
55. **Simmons, G., et al.** 2004. Characterization of severe acute respiratory syndrome-associated coronavirus (SARS-CoV) spike glycoprotein-mediated viral entry. Proc. Natl. Acad. Sci. U. S. A. **101:**4240–4245.
56. **Stertz, S., et al.** 2007. The intracellular sites of early replication and budding of SARS-coronavirus. Virology **361:**304–315.
57. **Szabo, R., S. Netzel-Arnett, J. P. Hobson, T. M. Antalis, and T. H. Bugge.** 2005. Matriptase-3 is a novel phylogenetically preserved membrane-anchored serine protease with broad serpin reactivity. Biochem. J. **390:**231–242.
58. **To, K. F., et al.** 2004. Tissue and cellular tropism of the coronavirus associated with severe acute respiratory syndrome: an in-situ hybridization study of fatal cases. J. Pathol. **202:**157–163.
59. **Voss, D., et al.** 2009. Studies on membrane topology, N-glycosylation and functionality of SARS-CoV membrane protein. Virol. J. **6:**79.
60. **Wang, P., et al.** 2004. Expression cloning of functional receptor used by SARS coronavirus. Biochem. Biophys. Res. Commun. **315:**439–444.
61. **Watanabe, R., et al.** 2008. Entry from the cell surface of severe acute respiratory syndrome coronavirus with cleaved s protein as revealed by pseudotype virus bearing cleaved s protein. J. Virol. **82:**11985–11991.
62. **Wong, S. K., W. Li, M. J. Moore, H. Choe, and M. Farzan.** 2004. A 193-amino acid fragment of the SARS coronavirus S protein efficiently binds angiotensin-converting enzyme 2. J. Biol. Chem. **279:**3197–3201.
63. **Wu, X. D., et al.** 2004. The spike protein of severe acute respiratory syndrome (SARS) is cleaved in virus infected Vero-E6 cells. Cell Res. **14:**400–406.
64. **Xiao, X., S. Chakraborti, A. S. Dimitrov, K. Gramatikoff, and D. S. Dimitrov.** 2003. The SARS-CoV S glycoprotein: expression and functional characterization. Biochem. Biophys. Res. Commun. **312:**1159–1164.
65. **Yang, Z. Y., et al.** 2004. pH-dependent entry of severe acute respiratory syndrome coronavirus is mediated by the spike glycoprotein and enhanced by dendritic cell transfer through DC-SIGN. J. Virol. **78:**5642–5650.
66. **Yang, Z. Y., et al.** 2004. A DNA vaccine induces SARS coronavirus neutralization and protective immunity in mice. Nature **428:**561–564.
67. **Yao, Y. X., J. Ren, P. Heinen, M. Zambon, and I. M. Jones.** 2004. Cleavage and serum reactivity of the severe acute respiratory syndrome coronavirus spike protein. J. Infect. Dis. **190:**91–98.